Monthly Notices
of the
ROYAL ASTRONOMICAL SOCIETY

MNRAS **494,** 2045–2052 (2020)
Advance Access publication 2020 April 14

doi:10.1093/mnras/staa790

An attempt to constrain Planet Nine's orbit and position via resonant confinement of distant TNOs

Brynna G. Downey [1]★ and Alessandro Morbidelli[2]

[1]*Department of Earth and Planetary Sciences, University of California Santa Cruz, 1156 High Street, Santa Cruz 95064, USA*
[2]*Laboratoire Lagrange, Universite Cote d'Azur, Observatoire de la Cote d'Azur, CNRS, CS 34229, F-06304 Nice, France*

Accepted 2020 March 17. Received 2020 February 13; in original form 2019 August 2

ABSTRACT

We considered four TNOs on elongated orbits with small semimajor axis uncertainties: Sedna, 2004 VN_{112}, 2012 VP_{113}, and 2000 CR_{105}. We found two sets of simultaneous near commensurabilities for these objects with a putative Planet Nine that are compatible with the current uncertainties in the objects' orbital periods. We conducted a large number of numerical simulations of quasi-coplanar simulations (i.e. inclinations of Planet Nine and TNOs set to zero but not the giant planets) to find which values of Planet Nine's mean anomaly and longitude of perihelion could put these objects in stable mean motion resonance (MMR) librations. We found no cases of simultaneous stable librations for multiple TNOs for more than 800 My, with most librations lasting much shorter than this time-scale. The objects 2004 VN_{112} and 2000 CR_{105} are the most unstable. Being in an MMR is not a strict requirement for long-term survival in 3D simulations, so our result cannot be used to refute Planet Nine's existence. Nevertheless, it casts doubt and shows that theoretical attempts to constrain the position of the planet on the sky are not possible.

Key words: celestial mechanics – Kuiper belt: general – planets and satellites: dynamical evolution and stability.

1 INTRODUCTION

Starting with the discovery of 2012 VP_{113} by Trujillo & Sheppard (2014), an alleged pattern arose in the known distant Trans-Neptunian Objects (TNOs) with $a > 150$ au, in which their arguments of perihelion (ω) seemed to cluster around $\sim 0^\circ$. There are no obvious orbital biases favouring the discovery of objects with $\omega \sim 0^\circ$ versus $\omega \sim 180^\circ$, so this observation called for a dynamical explanation, which the authors proposed could be the presence of a distant planet. Batygin & Brown (2016) noticed that for orbits with semimajor axis $a > 250$ au, the orbital clustering concerns not only the argument of perihelion but also the longitude of the node (Ω) and hence the longitude of perihelion (ϖ). In other words, the orbits are almost aligned with each other in physical space. Using simplified analytic models and numerical simulations, Batygin & Brown (2016) showed that an eccentric $\sim 10 M_\oplus$ perturber at a distance $a > 500$ au could generate an orbital clustering of distant TNOs over the lifetime of the Solar system and maintain it over time. The observed orbital clustering would be anti-aligned with the orbit of the planet itself, i.e. $\varpi - \varpi_{p9} \sim 180^\circ$, where ϖ_{p9} denotes the longitude of perihelion of this putative ninth planet of the Solar system. Since Batygin & Brown (2016), several further studies have tried to refine the predictions of Planet Nine's orbital parameters by analysing how the planet could maintain the TNOs in orbital confinement.

The quasi-2D numerical simulations of Batygin & Brown (2016) (i.e. particles starting with inclination $i = 0^\circ$, coplanar with Planet Nine and only the known giant planets having their real inclinations) and the finite inclination simulations of Batygin et al. (2019) found evidence for long-lasting TNOs on elongated orbits being trapped for a long time in mean-motion resonances (MMRs). Using 2D simulations, where all objects are coplanar, Batygin & Morbidelli (2017) showed that all bodies surviving for the age of the Solar system are in MMRs, although some can hop from one resonance to another during a short phase of instability. In full 3D simulations, with TNOs at their observed inclinations and Planet Nine at an inclination $i_{p9} = 20^\circ$–30°, the importance of MMRs for long-term survival is reduced because close encounters with Planet Nine are less frequent (Becker et al. 2017; Khain et al. 2018). Nevertheless, several objects spend significant time in resonances, and the final semimajor axis distribution of surviving objects clearly shows preference for resonant configurations (Becker et al. 2017).

Malhotra, Volk & Wang (2016) noticed that a Planet Nine with orbital semimajor axis $a_{p9} \sim 665$ au could put the six extreme TNOs known at the time (with $a > 150$ au and $q > 40$ au) near MMRs. They also put constraints on the planet's eccentricity to make these resonances stable. Millholland & Laughlin (2017)

★ E-mail: bgdowney@ucsc.edu

Table 1. Periods (yrs) and semimajor axes (au) with 1σ uncertainties of considered TNOs from JPL Small-Body Database and semimajor axes from Malhotra et al. (2016), labelled M16, and Millholland & Laughlin (2017), labelled ML17.

Object	P (JPL)	P 1σ (JPL)	a (JPL)	a 1σ (JPL)	a (M16)	a 1σ (M16)	a (ML17)
2000 CR_{105}	3307.22	14.44	221.98	0.64626	221.59	0.16	226.1
2012 VP_{113}	4242.42	32.43	262.07	1.3355	265.8	3.3	260.8
2004 VN_{112}	5910.63	47.54	326.91	1.7528	319.6	6.0	317.7
2010 GB_{174}	6586.69	715.78	351.38	25.462	350.7	4.7	369.7
Sedna	11430.27	21.10	507.42	0.62442	506.84	0.51	499.4

Table 2. TNO-Planet Nine MMRs for this work, Malhotra et al. (2016) and Millholland & Laughlin (2017). The first two of the MMR solutions, MMR1 and MMR2 end up being more stable and so are followed more in-depth. There are two 2000 CR_{105} solutions in MMR3, which adds no complexity since 2000 CR_{105} was too unstable to give meaningful constraints in our simulations.

TNO	MMR1	MMR2	MMR3	MMR4	MMR5	MMR6	M16	ML17
2000 CR_{105}	9:2	9:1	7:3 or 9:4	3:1	9:2	3:2	5:1[a]	5:1
2012 VP_{113}	7:2	7:1	9:5	7:3	7:2	7:6	4:1	4:1
2004 VN_{112}	5:2	5:1	9:7	5:3	5:2	5:6	3:1	3:1
Sedna	4:3	8:3	2:3	6:7	9:7	3:7	3:2	3:2
a_{p9}	615 au	976 au	387 au	458 au	600 au	288 au	665 au	654 au

[a]Malhotra et al. (2016) deemed 2000 CR_{105} too far outside the error bounds to really be in the 5:1 MMR resonance with Planet Nine.

similarly searched for low-order Planet Nine-TNO resonances and derived a semimajor axis probability distribution for Planet Nine, as well as probability distributions for the other orbital elements. The most prominent peak of the probability distribution corresponded to $a_{p9} \sim 654$ au, $e_{p9} \sim 0.4$–0.5, $\Omega_{p9} \sim 50^\circ$, $\omega_{p9} \sim 150^\circ$, and $i_{p9} \sim 30$–40°.

This paper builds off of the ideas of Malhotra et al. (2016) and Millholland & Laughlin (2017) but with notable differences. Most importantly, we look for orbital configurations that minimize the libration amplitude of the resonant angles, unlike previous works that checked the libration of these angles only a posteriori. Because the mean longitudes and longitudes of perihelion of the TNOs are well constrained by observations, whereas their semimajor axes (and hence orbital periods) have large errors, checking the actual libration of the resonant angles is a much more severe test for possible simultaneous resonant configurations than simply looking at orbital period ratios.

This paper is structured as follows. In Section 2, we look at orbital period ratios among the TNOs on elongated orbits to see which resonances with Planet Nine are potentially real. In Section 3, we describe the simulations that we have conducted and how we analysed them to find values of the planet's mean anomaly and longitude of perihelion that can put all the TNOs in long-term MMR libration. In Section 4, we present our results, and their significance for the Planet Nine problem is discussed in Section 5.

2 TNO-P9 RESONANCES FROM TNO PERIOD UNCERTAINTIES

If Planet Nine is keeping the distant TNOs in MMRs, then these TNOs should have apparent mean-motion commensurabilities with each other, within their orbital period uncertainties. In this section, we look for these commensurabilities and derive possible orbital semimajor axes for Planet Nine.

Four TNOs were used with $a > 200$ au: Sedna (90377), 2004 VN_{112}, 2012 VP_{113}, and 2000 CR_{105} (148209). We did not consider 2010 GB_{174} because its semimajor axis uncertainty of 25 au was too high to make it a useful constraint.

Following a suggestion by S. Chesley, we used the barycentric orbital elements of the distant TNOs. The barycentric elements are more constant over time, while the heliocentric elements vary due to the rotation of the Sun relative to the Solar system's barycenter, mostly associated to the orbital motion of Jupiter. Each TNO's barycentric orbital elements came from the JPL HORIZONS Web-Interface[1] and the element uncertainties from the JPL Small-Body Database Browser[2]. The semimajor axes and periods are listed in Table 1 along with the barycentric semimajor axes used in Malhotra et al. (2016) from their own orbit-fitting software. Millholland & Laughlin (2017) used the heliocentric elements from the JPL Small-Body Database, which differed by 2–9 au in semimajor axis from the barycentric elements. The difference in using heliocentric versus barycentric elements alone can explain the difference in resonances found between Millholland & Laughlin (2017) and this work. The comparison between the JPL Small-Body Database elements and those from orbit-fitting software highlights the fact that elements for long-period bodies in our Solar system vary greatly from data base to data base, with one potentially being outside of the 1σ bounds of another. Also, the orbital elements are refined over time by more observations. A common argument is that the Planet Nine problem will become clearer with further discoveries of distant Solar system objects, but obtaining consistent and precise values for the orbital elements of the known TNOs would also help.

The logic for finding TNO–TNO resonances and TNO-P9 resonances went as follows. If Planet Nine were in MMRs with the distant TNOs, then the TNOs should be in apparent resonances with each other, and this should be detectable in their orbital period

[1]https://ssd.jpl.nasa.gov/horizons.cgi
[2]https://ssd.jpl.nasa.gov/sbdb.cgi

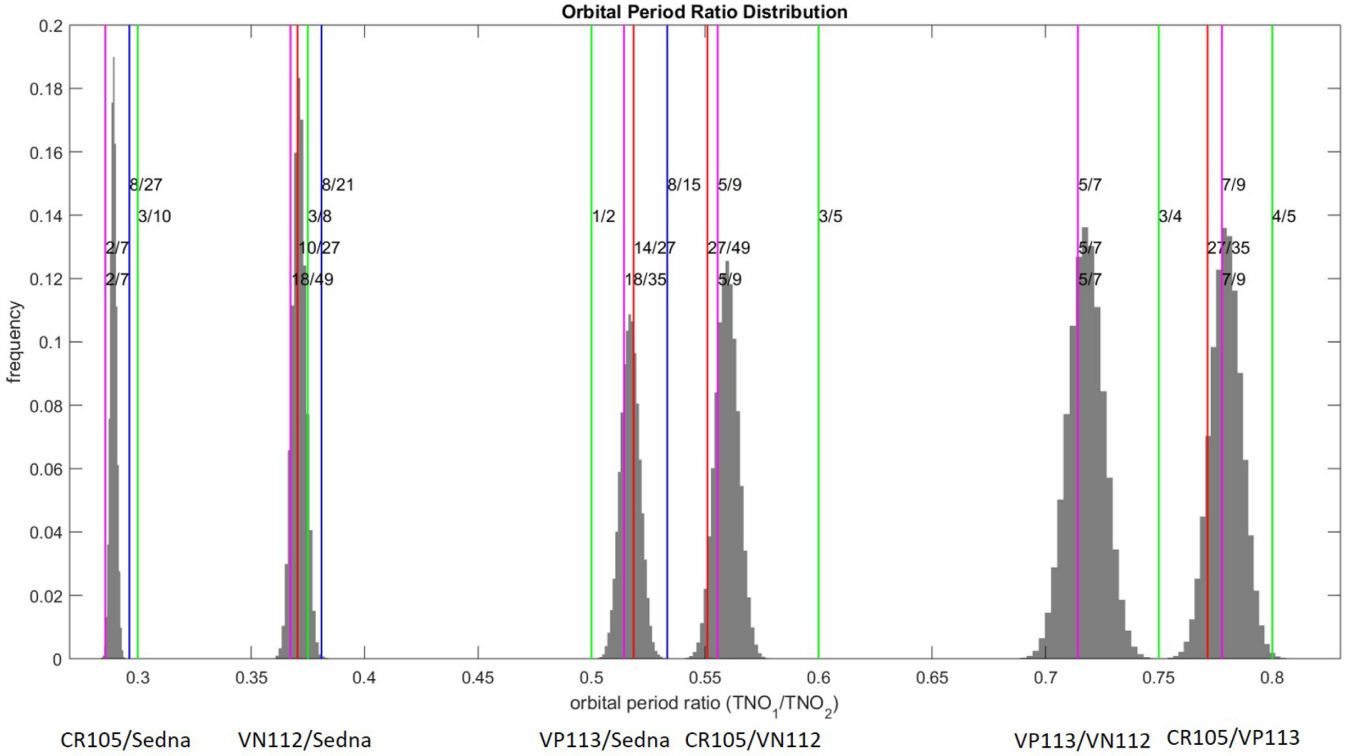

Figure 1. Period ratio distribution for each TNO pair in grey. The location of the proposed TNO–TNO period resonances are plotted as lines. MMR1 and MMR2 from Table 2 (the more likely resonances) are the blue lines, MMR3 are red (MMR3 has two possible solutions for 2000 CR_{105}, so the 7:3 MMR is plotted), MMR4-6 are magenta, and those of Millholland & Laughlin (2017) and Malhotra et al. (2016) are green. Note that some of the lines overlap, for example MMRs1-2 and MMRs4-6 overlap for 2000 CR_{105}/2004 VN_{112} and 2000 CR_{105}/2012 VP_{113}, and all but the Millholland & Laughlin (2017) lines overlap for 2012 VP_{113}/2004 VN_{112}. For the more likely scenarios, Sedna:P9 is 4:3 or 8:3, 2004 VN_{112}:P9 is 5:2 or 5:1, and 2012 VP_{113} is 7:2 or 7:1. For Millholland & Laughlin (2017), Sedna:P9 is 3:2, 2004 VN_{112}: P9 is 3:1, and 2012 VP_{113} is 4:1.

ratios. Given the uncertainties in semimajor axes, each TNO has a period probability distribution, so each TNO pair has a period ratio distribution. Rational numbers are a dense set, so one can find an infinite number of potential commensurabilities falling within each period ratio distribution. However, each TNO–TNO period ratio has to be the quotient of each considered TNO's period with Planet Nine's, i.e. $P_{\mathrm{TNO_a}}/P_{\mathrm{p9}} \times P_{\mathrm{p9}}/P_{\mathrm{TNO_b}} = P_{\mathrm{TNO_a}}/P_{\mathrm{TNO_b}}$. To ensure that these are low-integer ratios and that Planet Nine is farther away than the TNOs, the $P_{\mathrm{TNO}}/P_{\mathrm{p9}}$ period ratio was searched among the values M/N where $M < 5$, $N < 10$, $M < N$. Sifting through all $M < 5$, $N < 10$, each potential $P_{\mathrm{TNO_a}}/P_{\mathrm{TNO_b}}$ ratio of the form $(M_1/N_1)/(M_2/N_2) = M_1N_2/N_2M_1$ was checked to see if it fell within the $P_{\mathrm{TNO_a}}/P_{\mathrm{TNO_b}}$ period ratio distribution.

We found two sets of TNO-P9 ratios for the same set of $P_{\mathrm{TNO_a}}/P_{\mathrm{TNO_b}}$ ratios, which are listed in Table 2 under MMR1 and MMR2 along with the MMRs found for Malhotra et al. (2016) and Millholland & Laughlin (2017). The TNO period ratio distributions and the proposed resonances are depicted in Fig. 1 in blue. The first of our solutions would put Planet Nine at $a_{\mathrm{p9}} = 615$ au, and the second at $a_{\mathrm{p9}} = 976$ au. Given that the preferred a_{p9} in Batygin et al. (2019) is 400–800 au, the first solution would fit with their simulation predictions and those of Malhotra et al. (2016) and Millholland & Laughlin (2017), whereas the second is outside of most prediction bounds.

We notice from Fig. 1 that our preferred resonant configuration fits the period ratio between 2012 VP_{113} and 2004 VN_{112} better than those previously proposed. For the 2004 VN_{112}/Sedna period ratio, both ours and previous resonant choices fall at the margin of the period-ratio distribution. For the 2012 VP_{113}/Sedna period ratio, our preferred resonance is slightly farther from the nominal ratio than that proposed in Millholland & Laughlin (2017), but still falls within the period ratio distribution. On the other hand, the period ratios involving 2000 CR_{105} are much better reproduced by our preferred resonances than those proposed in Millholland & Laughlin (2017). In particular, the resonant configuration of Millholland & Laughlin (2017) falls off the period ratio distribution for the 2000 CR_{105}/2004 VN_{112} pair.

The resonances mentioned up to this point assumed that Planet Nine was beyond the farthest TNO we considered, Sedna, and was in low-order resonances with all TNOs. Four more resonances were investigated with one having a high-order $P_{\mathrm{p9}}/P_{\mathrm{Sedna}}$ resonance and three with $P_{\mathrm{p9}} < P_{\mathrm{Sedna}}$. For the high-order Sedna resonance, Planet Nine was simulated with a mass of $10M_{\oplus}$ like before, but for the other three resonances, following Batygin (private communication), it was assigned a mass of $5M_{\oplus}$. These resonances are listed in Table 2 as MMRs3-6 and are plotted in Fig. 1 in red for MMR3 and in magenta for MMRs4-6. Note that different TNO-P9 resonances lead to the same TNO–TNO resonances in MMRs4-6. The corresponding TNO–TNO resonant lines for MMRs3-6 are closer to the central peaks of the period ratio distributions than for MMRs1-2 in all distributions of period ratios with Sedna. Furthermore, three out of these four resonances, MMRs 3-5, are within or very near the preferred $a_{\mathrm{p9}} = 400$–800 au range in Batygin et al. (2019).

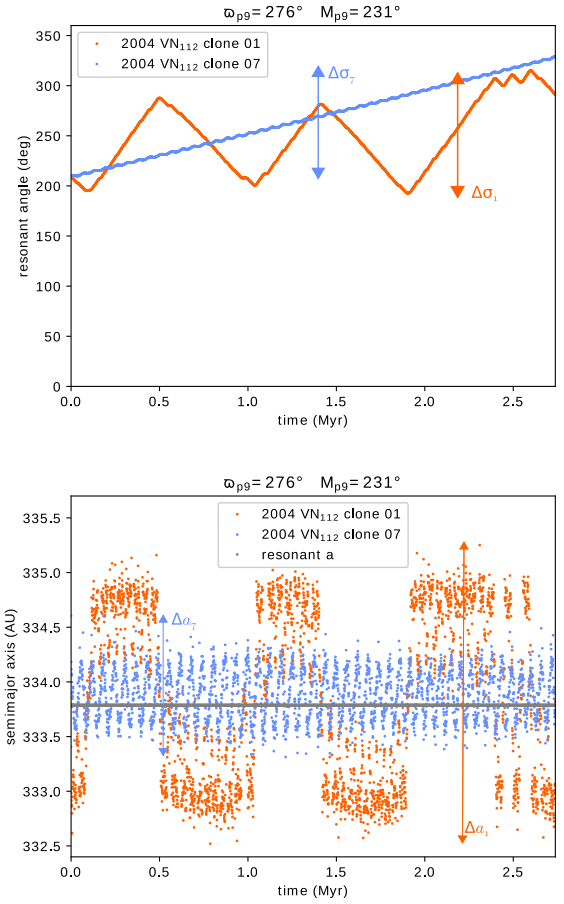

Figure 2. An example of how the resonant angle (top) and semimajor axis (bottom) amplitudes of oscillation were calculated for each TNO clone over the considered 10^9 d (2.7 Myr) timespan. This example is from the MMR2 solution, so $a_{p9} = 976$ au. In the bottom panel, both clones clearly librate about the 5:1 resonance, which is marked in grey for reference.

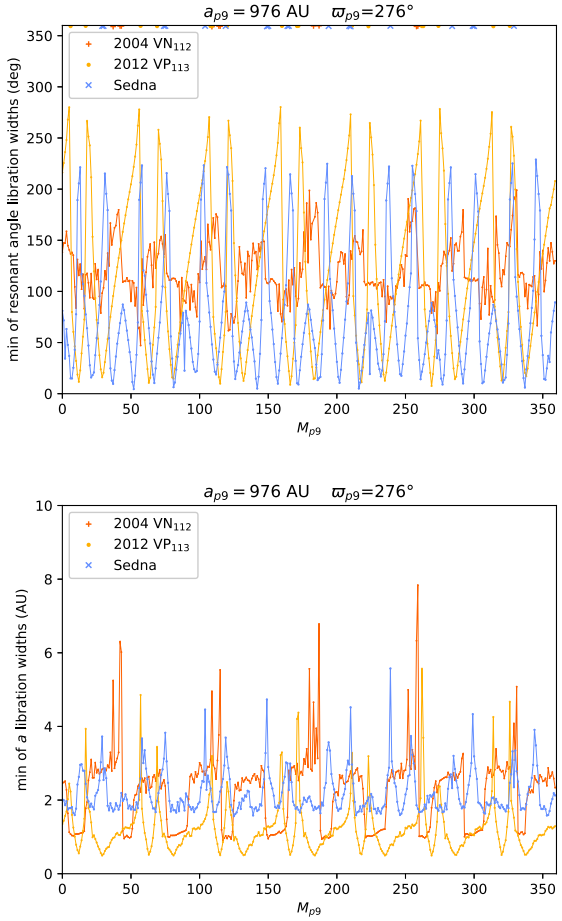

Figure 3. The minimum amplitudes of oscillation for the resonant angle (top) and semimajor axis (bottom) for 2004 VN_{112}, 2012 VP_{113}, and Sedna as a function of Planet Nine's mean anomaly. They are the minima of 10 clones that were initialized at different semimajor axes above and below the resonant value. $a_{p9} = 976$ au, $\varpi_{p9} = 276^\circ$ (initialized anti-aligned to Sedna's ϖ), and the integration time is 10^9 d (2.7 Myr). Clear peaks and troughs indicate that resonance angle confinement for Sedna and 2012 VP_{113} is periodic in Planet Nine's mean anomaly.

3 SIMULATIONS SEARCHING FOR RESONANCE EVIDENCE

We did a suite of simulations searching for long-term resonance stability of the TNOs for the two resonant semimajor axes of Planet Nine, corresponding to MMR1 and MMR2 from Table 2, while varying Planet Nine's longitude of perihelion and mean anomaly. The *N*-body simulations were done using the SWIFT package with the four known giant planets and the putative fifth outer planet. A multidimensional parameter search being unfeasible, the following parameters were fixed: $e_{p9} = 0.7$, $i_{p9} = 0^\circ$, and $m_{p9} = 10M_\oplus$. The free parameters of Planet Nine are therefore just its longitude of perihelion, ϖ_{p9}, and mean anomaly, M_{p9} (its semimajor axis, a_{p9}, was fixed to either 615 au or 976 au). For simplicity, we investigated the planar problem, where the inclinations of the TNOs and Planet Nine were set equal to zero but not for the four giant planets whose inclinations were kept. For each TNO, we considered 10 clones to sample the semimajor axis probability distribution by fixing a range from −1 au to +1 au from the nominal resonant semimajor axis, of the order of the 1σ uncertainties reported in Table 1. For the TNOs' orbital angles ϖ and M, we adopted the nominal parameters, given that for these angles the observational errors are small. We also adopted the nominal TNOs' eccentricities, even if they are uncertain, because the value of the eccentricity should not significantly affect the ability of the resonant angle to be in libration, which is our test for a possible resonant configuration.

The eccentricity adopted for Planet Nine ($e_{p9} = 0.7$) is a ballpark estimate from earlier works (Batygin & Brown 2016). The same authors have now concluded from further simulations that e_{p9} is closer to the range 0.2–0.5, but this was not known at the time of this study (Batygin et al. 2019).

As for the TNO eccentricity, the value of e_{p9} is likely to influence the resonance width, but it should not significantly influence the libration ability of the resonant angles of the TNO clones. Remember, however, that Malhotra et al. (2016) found that the coplanar 5:2 resonance is stable only for $e_{p9} < 0.18$. In our first solution, MMR1, 2004 VN_{112} is in the 5:2 resonance with Planet Nine and therefore the large value of e_{p9} that we assumed may be the reason for the unstable behaviour that will be observed below. Had we used $e_{p9} = 0.2$–0.5 as in Batygin et al. (2019), 2004 VN_{112}'s 5:2 resonance would have still been unstable. On the other hand, a value of $e_{p9} < 0.18$ is difficult to explain in the framework of the main scenarios proposed to explain the existence of Planet Nine: either the capture from another planetary system during a stellar flyby (Jílková et al. 2015, 2016; Mustill, Raymond & Davies

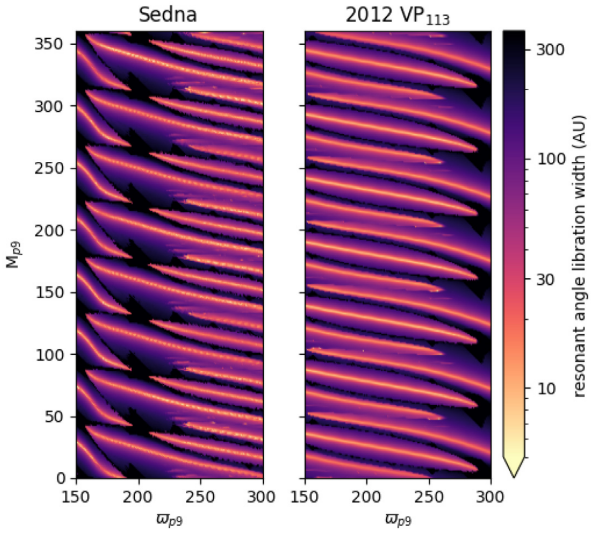

Figure 4. The minimum amplitudes of oscillation for the resonant angles of Sedna and 2012 VP_{113} as a function of M_{p9} and ϖ_{p9}. $a_{p9} = 976$ au and $\varpi_{p9} = 150^\circ$–300° to encompass values that represent anti-alignment to the considered TNOs. Fig. 3 would be a cross-section of this figure. The resonant angle is used to narrow down possible Planet Nine configurations because it has a well-defined periodic behaviour. 2004 VN_{112} is not included because its pattern is more chaotic. We narrowed down possible M_{p9} and ϖ_{p9} first with Sedna and 2012 VP_{113} and added 2004 VN_{112} in after.

2016) or the ejection from the giant planet region of the Solar system followed by a partial circularization due to the gravitational field of the stellar cluster in which the Sun presumably formed (Morbidelli & Levison 2004; Izidoro et al. 2015; Batygin & Brown 2016).

We conducted a large number of simulations. For each simulation, with given values of M_{p9} and ϖ_{p9}, 10 clones of Sedna, 2004 VN_{112}, and 2012 VP_{113} were evolved over 10^9 d or 2.7 Myr. For simplicity, we did not simulate 2000 CR_{105}, looking first for a resonant configuration of the first three objects, as they are on more elongated orbits.

The range of values of ϖ_{p9} that we explored was meant to cover the values corresponding to anti-alignment with Sedna, 2004 VN_{112}, and 2012 VP_{113}, which are 276°, 213°, and 205°, respectively. Thus, the range $\varpi_{p9} = 150$–300° was adopted with an interval of 1°. For each ϖ_{p9} value, the full 360° circle in mean anomaly M_{p9} was tested also with an interval of 1°.

In order to automate the analysis of this very large number of simulations, the amplitude of oscillation in semimajor axis and resonant angle were calculated for each clone as shown in Fig. 2. The resonant angle was the one of the form $\sigma_{TNO} = n\lambda_{TNO} - m\lambda_{p9} - (n-m)\varpi_{TNO}$, where $\lambda = \varpi + M$, and n:m is the TNO:Planet Nine MMR. In reality, there are several resonant angles with different combinations of ϖ_{TNO} and ϖ_{p9} instead of $(n-m)\varpi_{TNO}$ (Batygin & Morbidelli 2017), but, because the period of $\varpi_{TNO} - \varpi_{p9}$ is much longer than that of the resonant angles, if one resonant angle librates then all librate.

The minimum amplitude of oscillations of a_{TNO} and σ_{TNO} among the 10 TNO clones was taken as representative amplitudes for that simulation and that TNO. Some clones did not survive the simulation due to close encounters with either Neptune or Planet Nine, so these were discarded in the computation of the representative amplitudes.

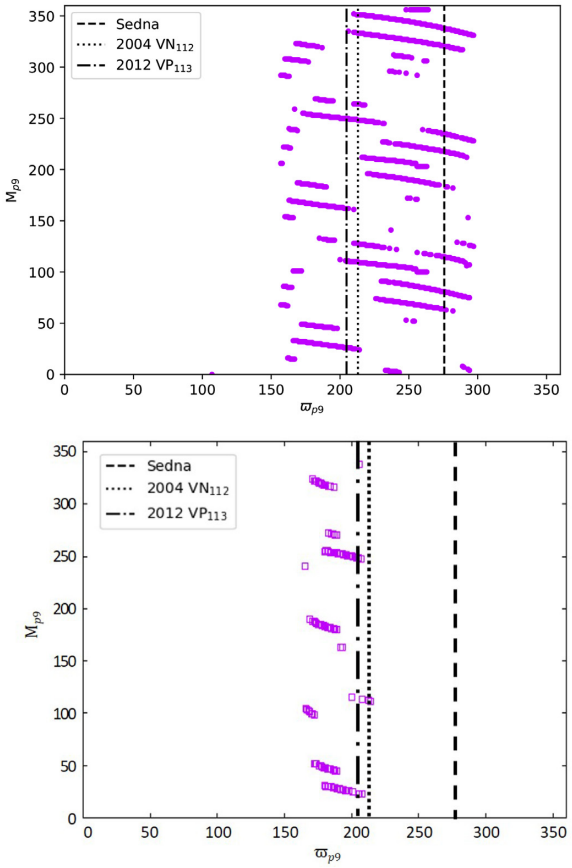

Figure 5. The top panel is the intersection of the local minima of Sedna and 2012 VP_{113} from Fig. 4. These points were tested for long-term TNO stability. The bottom panel are those points in the top panel where 2004 VN_{112} had deviated by less than 10 au in semimajor axis after 10^{11} d (273.8 Myr). The vertical lines mark the ϖ_{p9} corresponding to initialized anti-alignment to 2004 VN_{112}, 2012 VP_{113}, and Sedna. The longer lasting runs cluster around anti-alignment to 2004 VN_{112} and 2012 VP_{113}.

Fig. 3 shows the representative amplitudes for each TNO (shown in different colours) as a function of Planet Nine's mean anomaly for $\varpi_{p9} = 276^\circ$. The top panel refers to the representative amplitude of the resonance angle and the bottom panel the semimajor axis. Fig. 4 takes the representative amplitudes for Sedna and 2012 VP_{113} for all M_{p9} over the range $\varpi_{p9} = 150^\circ - 300^\circ$ to elucidate the periodic patterns in the libration widths.

In principle, smaller amplitudes of oscillation mean more constrained dynamics in that there is a higher chance to librate deep in the MMR. In particular, if a body is far from resonance, its resonance angle circulates fully within the integration time-scale, so its amplitude is 360°. A small amplitude of the critical angle means that the angle is either in narrow libration or it has a slow motion (see Fig. 2). Both behaviours indicate close proximity to the considered resonance. Thus, the desired Planet Nine configuration is the one where all TNOs have the smallest representative amplitudes. This occurs at the minima of the values in Fig. 4, which are plotted in the top panel of Fig. 5 for Sedna and 2012 VP_{113}. For 2004 VN_{112}, the minima are not as well defined (see Fig. 3), so we decided to concentrate on where the minima for Sedna and 2012 VP_{113} intersect shown in the top panel of Fig. 5. In other words, we isolated the values of M_{p9} and ϖ_{p9} that simultaneously minimize the representative amplitudes of oscillation of both of these objects.

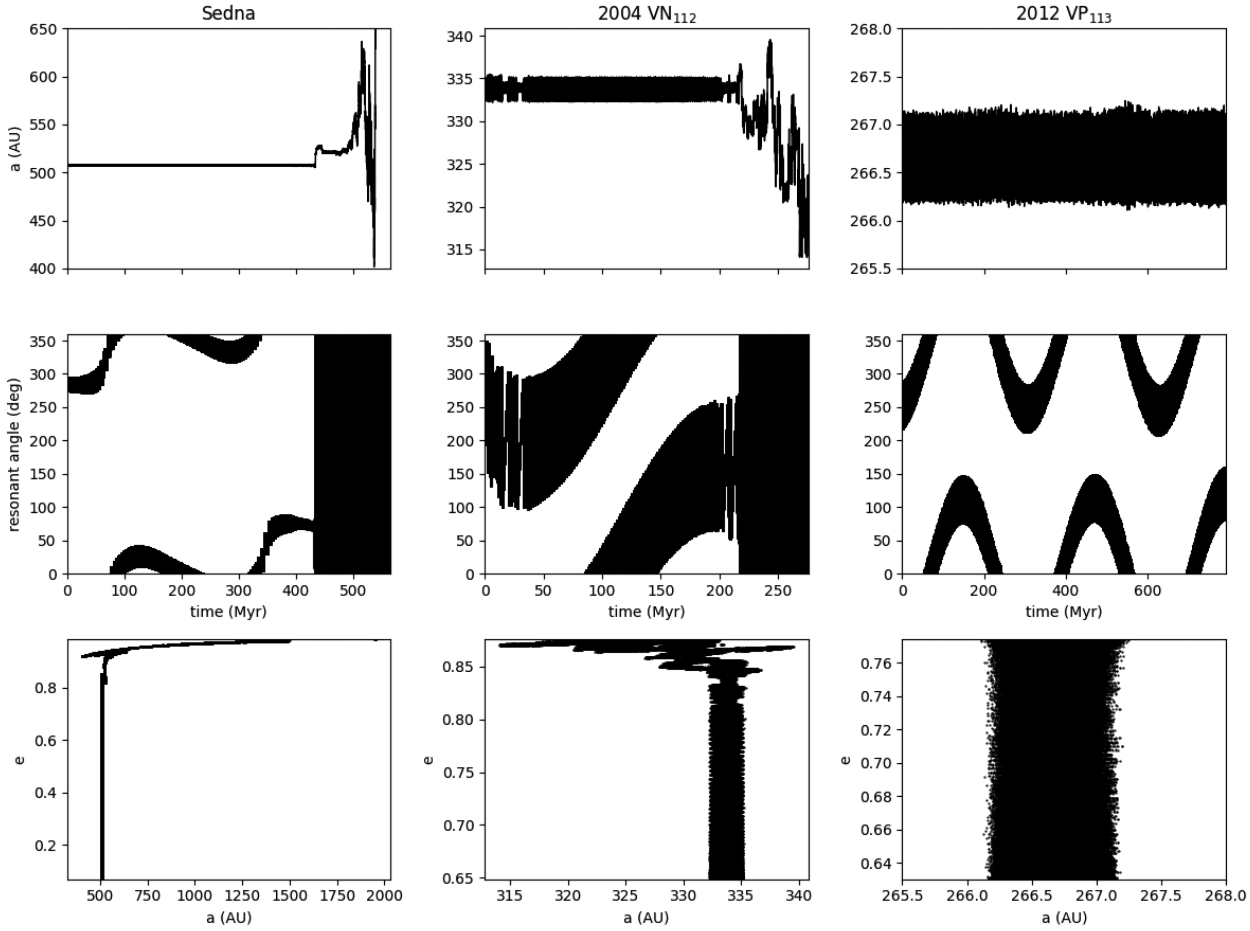

Figure 6. Examples of long-term orbital evolution of Sedna (left), 2004 VN_{112} (middle), and 2012 VP_{113} (right) in the presence of Planet Nine at 976 au for $M_{p9} = 180^\circ$ and $\varpi_{p9} = 186^\circ$. Sedna and 2004 VN_{112} eventually become unstable; the critical angles start circulating and the semimajor axis shows evidence of close encounters. 2012 VP_{113} remains stable and in resonance for the duration of the simulation (821.4 Myr).

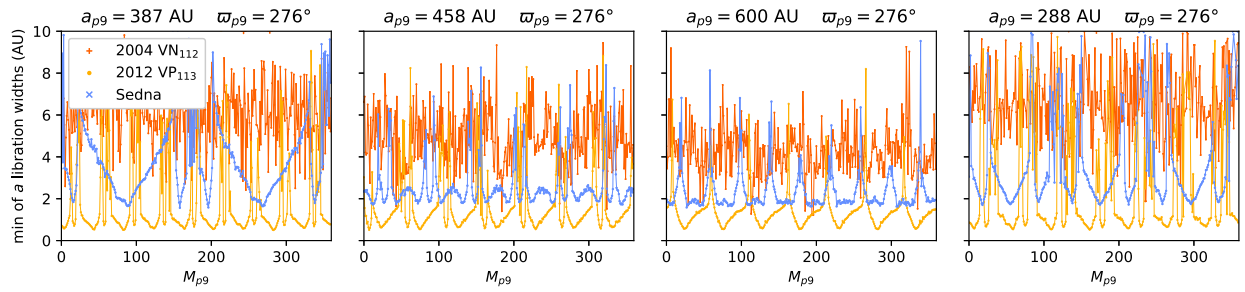

Figure 7. The minimum semimajor axis libration widths of all TNO clones (same as Fig. 3) but for the resonances listed in Table 2 under MMRs3-6 from left to right, respectively. The resonant angle widths were mostly 360° for 2004 VN_{112}, so the semimajor axis widths provided more information on how these resonances fared.

We did longer simulations of 10^{11} d (273.8 Myr) for these Planet Nine configurations, monitoring chiefly 2004 VN_{112} since Sedna and 2012 VP_{113} had already been proven to be stable. Of these Planet Nine configurations, we selected those for which the change in the resonant semimajor axis of 2004 VN_{112} was less than 10 au on this timespan (the bottom panel of Fig. 5). The result was a list of configurations that showed long-term stability for all three objects.

4 RESULTS

In the case of Planet Nine at $a_{p9} = 615$ au, no clones of 2004 VN_{112} had a resonant semimajor axis evolution confined within 10 au over the long (273.8 Myr) simulation. This means that it is not possible, for any value of M_{p9} and ϖ_{p9} to keep Sedna, 2012 VP_{113} and 2004 VN_{112} simultaneously in a stable resonant configuration. When Sedna and 2012 VP_{113} seem to have a stable resonant motion, 2004 VN_{112} is strongly unstable. This is not surprising. As reported

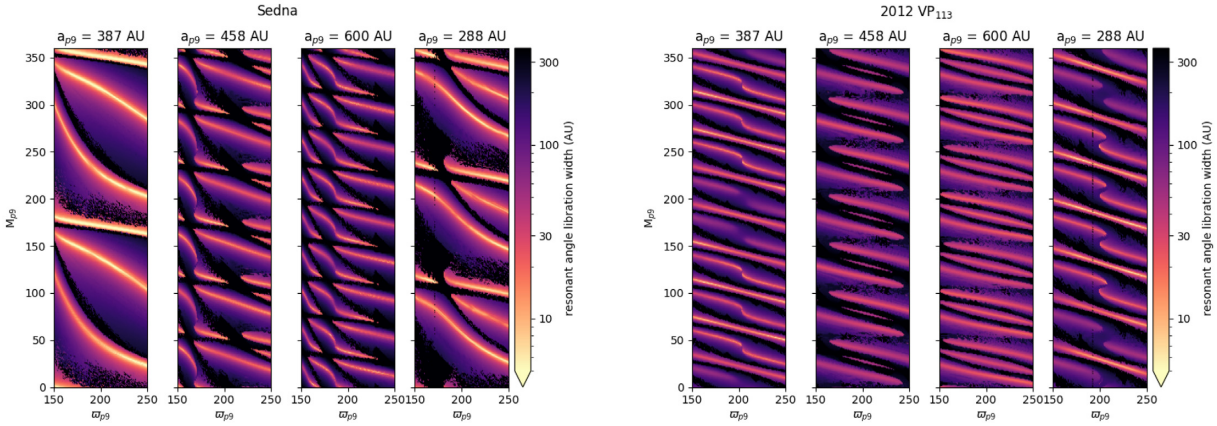

Figure 8. The same as Fig. 4 but for $\varpi_{\rm p9} = 150$–250° and for resonances MMRs3-6 in Table 2. The periodic patterns are less linear than for MMR2 with more abrupt changes in Sedna's libration widths, perhaps indicating lower stability.

above, for this value of $a_{\rm p9}$, 2004 $\rm VN_{112}$ would be in the 5:2 MMR with the planet and this is unstable for $e_{\rm p9} > 0.18$ (Malhotra et al. 2016).

In the case with $a_{\rm p9} = 976$ au, we found several configurations ($M_{\rm p9}$, $\varpi_{\rm p9}$) near the minima of the oscillation amplitudes of Sedna and 2012 $\rm VP_{113}$ where the semimajor axis of 2004 $\rm VN_{112}$ remained confined within 10 au. These configurations are shown in the bottom panel of Fig. 5. These configurations are spread out in $M_{\rm p9}$ but are confined within the range of $165^\circ < \varpi_{\rm p9} < 214^\circ$.

Unfortunately, none of these configurations proved to be really stable on a longer 3×10^{11} d (821.4 Myr) time-scale. Not only 2004 $\rm VN_{112}$ but Sedna as well showed instabilities. Only 2012 $\rm VP_{113}$ remained stable throughout the full simulation duration for most of the considered configurations. Fig. 6 shows an example of the long-term evolution of one of the considered initial configurations. Both Sedna and 2004 $\rm VN_{112}$ eventually exit from their respective resonances (the resonant angle starts to circulate). This triggers close encounters with the planet, revealed by the stochastic changes in their semimajor axes, which is particularly visible for Sedna. We also did simulations of the behaviour of 2000 $\rm CR_{105}$ for the same ($M_{\rm p9}$, $\varpi_{\rm p9}$) configurations but we found that the motion of this object is always strongly unstable.

To cover our bases, we also checked the resonances in Table 2 under MMRs3-6, which are either interior to Sedna or are higher order, meaning Planet Nine is less likely to be in these configurations. Fig. 7 shows plots analogous to the bottom panel of Fig. 3 but for MMRs3-6. In contrast to MMRs1-2, these have a less sharp peak and trough pattern. Fig. 8 shows plots analogous to Fig. 4. The periodic patterns are less linear than for MMR2, potentially indicating their lower stability. Repeating the analysis described above, we found no configurations with semimajor axes remaining confined within 10 au for more than 10^{10} d (27.4 Myr). Again, 2004 $\rm VN_{112}$ is the body most prone to instability.

5 DISCUSSION

In this work, we have tried to find an orbit for the putative Planet Nine and its current position on the orbit that leads to a long-term resonant stabilization of the motion of the TNOs with very elongated orbits: Sedna, 2004 $\rm VN_{112}$, and 2013 $\rm VP_{113}$. A planet configuration that puts simultaneously three objects in resonance would not be trivial and finding it would give great confidence to the existence of Planet Nine and even help constrain its position in the sky.

Unfortunately, our attempts have been unsuccessful. It does not seem possible (or at least we did not find the correct configuration) to put the three considered TNOs simultaneously in long-term stable resonances. The longest resonant configurations we found lasted less than 800 My.

Although discouraging, our results may not mean the end for Planet Nine. Resonant confinement for the survival of the distant TNOs over the age of the Solar system is mandatory in 2D models, such as the one we considered. In fact, in this case the lack of resonant configuration very rapidly leads to destabilizing close encounters between the TNO and Planet Nine (Batygin & Morbidelli 2017). However, in 3D models and particularly if the mutual inclinations between the TNOs and Planet Nine are not small, close encounters may be avoided in the long-term even without mean-motion resonant confinement. In this case, not finding all distant TNOs in resonance with the planet today may not be a fatal problem.

Becker et al. (2017) performed 3D simulations of TNOs with Planet Nine on different orbital configurations and they emphasized that even long-lasting TNOs show significant diffusion in semimajor axis. Several objects spend significant time in resonances (see their Fig. 8) and the final semimajor axis distribution of surviving objects clearly shows preference for resonant configurations (see their fig. 7). Nevertheless, this does not imply that the objects have to be all in resonance at the present time and forevermore.

Beust (2016) was the first to suggest that the confinement of the longitudes of perihelion could just be the consequence of the secular interaction between the TNOs and Planet Nine, without the need of MMRs to be involved. In fact, Hadden et al. (2018) showed that TNOs maintained long-term anti-alignment with Planet Nine while chaotically diffusing in semimajor axis. This diffusion was nevertheless characterized by temporary captures in MMRs. Clearly, MMRs are not needed for the clustering in longitude of perihelion but they help for the long-term survival of the objects.

However, the lack of a clear MMR signature prevents us from constraining the planet's orbit and position on the orbit, which would have guided the observational efforts for its discovery. Secular dynamics alone cannot provide any information on the planet's mean anomaly. Thus, if most TNOs are not in an MMR today with Planet Nine, it becomes impossible to infer theoretically the current

position of the planet in the sky. Actually, for the latest results, all attempts to use theoretical analyses to characterize even just the orbit of Planet Nine (i.e. leaving aside its position) failed to provide significantly strict bounds.

The situation may be reminiscent of that of the early 1900s, when it was believed that an unknown Planet X was responsible for anomalies in the motion of Neptune. Unlike the case of Uranus that led to the discovery of Neptune, no theoretical analysis led by even the brightest minds of the epoch converged to any prediction of Planet X's position. Pluto's discovery was pure serendipity, for we know today that Pluto is too small to cause any visible perturbations in Neptune. In fact, the anomalies in the motion of Neptune that the astronomers of the time thought they had detected were not real (Standish 1993). Is history repeating itself today? The distribution of the orientations of the elongated TNO orbits does not seem to evolve towards a more uniform distribution as more objects are found. The recent orbital determination of 2015 TG_{387} 'Goblin' (Sheppard et al. 2018) reinforces the appearance that the most elongated TNO orbits are quasi-aligned with each other (Trujillo & Sheppard 2014; Batygin & Brown 2016; Brown & Batygin 2016). Observational biases have been proposed to be the cause of this apparent non-uniform distribution of longitude of perihelion (Shankman et al. 2017), but a re-analysis of large-area surveys suggests that this is not the case (Brown & Batygin 2016). The discovery of 2015 BP_{519} (Becker et al. 2017) on a high-inclination, large perihelion-distance orbit, lying on an orbital track towards retrograde inclinations predicted in Batygin & Morbidelli (2017), also feeds the hope that Planet Nine exists and will be eventually found. There are many more arguments for and against the existence of Planet Nine, which are discussed in-depth in the Batygin et al. (2019) review after taking into account more subtle dynamics that are not considered here.

Given the lack of theoretical guiding, likely only an all-sky deep survey like LSST's will be able to give the last word on Planet Nine.

ACKNOWLEDGEMENTS

BGD would like to acknowledge the MIT MISTI-France programme for partial support of this project at OCA. We acknowledge use of the lux supercomputer at UC Santa Cruz, funded by NSF MRI grant AST 1828315.

REFERENCES

Batygin K., Brown M. E., 2016, AJ, 151, 22
Batygin K., Morbidelli A., 2017, AJ, 154, 229
Batygin K., Adams F. C., Brown M. E., Becker J. C., 2019, Phys. Rep., 805, 1
Becker J. C., Adams F. C., Khain T., Hamilton S. J., Gerdes D., 2017, AJ, 154, 61
Beust H., 2016, A&A, 590, L2
Brown M. E., Batygin K., 2016, ApJ, 824, L23
Hadden S., Li G., Payne M. J., Holman M. J., 2018, AJ, 155, 249
Izidoro A., Morbidelli A., Raymond S. N., Hersant F., Pierens A., 2015, A&A, 582, A99
Jílková L., Portegies Zwart S., Pijloo T., Hammer M., 2015, MNRAS, 453, 3157
Jílková L., Hamers A. S., Hammer M., Portegies Zwart S., 2016, MNRAS, 457, 4218
Khain T. et al., 2018, AJ, 156, 273
Malhotra R., Volk K., Wang X., 2016, ApJ, 824, L22
Millholland S., Laughlin G., 2017, AJ, 153, 91
Morbidelli A., Levison H. F., 2004, AJ, 128, 2564
Mustill A. J., Raymond S. N., Davies M. B., 2016, MNRAS, 460, L109
Shankman C. et al., 2017, AJ, 154, 50
Sheppard S., Trujillo C., Tholen D., Kaib N., 2018, AJ, 157, 139, preprint (arXiv:1810.00013)
Standish E. M., 1993, AJ, 105, 2000
Trujillo C. A., Sheppard S. S., 2014, Nature, 507, 471

This paper has been typeset from a TEX/LATEX file prepared by the author.